Annals of R.S.C.B., ISSN:1583-6258, Vol. 26, Issue 1, 2022, Pages. 1077- 1092
Received 08 November 2021; Accepted 15 December 2021.

Three Dimensional Fluorescence Spectral Analysis on the Binding Interaction of Alizarin Red Dye in Reverse Micelle

L. Anni Bebin, H. Dhilshath Raihana, K. Swarnalatha*
Department of Chemistry, Manonmaniam Sundaranar University, Abishekapatti, Tirunelveli-12, Tamil Nadu
*swarnalatha@msuniv.ac.in

ABSTRACT

In this work, we have focused on the photophysical properties of Alizarin red dye (Sodium salt of 1,2-dihydroxy-9,10-anthraquinone-3-sulfonic acid) in reverse micelle, particularly anionic micelle, AOT. Binding interactions of Alizarin Red Dye in AOT reverse micelles are analyzed using two dimensional (2D) (steady state) fluorescence and three dimensional (3D) fluorescence spectroscopy. On increasing the size of water pool (W_0 from 0 to 60), there was considerable enhancement in the absorption as well as fluorescence intensity with red shift indicated that the alizarin red dyes confined in the core of the reverse micelles and has a strong interaction with the sulfonate head group. Fluorescence technique was used. The binding parameters (binding sites, ~ 1 (0.94) and binding constant, 3.395 X 10^4 M^{-1}), quantum yield (0.074), partition coefficient (6.5 X 10^4), excited state pKa value (6) are determined with the aid of fluorescence technique. The observed results suggest that the fluorescence spectral analysis can be successfully used to study the binding interaction of any type of dyes in microheterogeneous media.

Keywords Alizarin red, AOT reverses micelle, two and three dimensional, fluorescence technique

Introduction

The nanometric surfactant aggregates (reverse micelles) received greater engrossment among researchers during recent times, on account of its unlocking pathways for biological membrane models, molecular delivery systems and quantum dot templating, etc [1- 2]. When nanoscaled droplets of a hydrophilic solvent (generally water – like phase) is trapped into amphiphilic surfactant shell, self assemble them in a spherical supramolecular system resulted into reverse or inverted micelles (RMs). They are thermodynamically stable, optically transparent, isotropic, wherein hydrophilic-hydrophobic moiety obtained towards inner polar-outer nonpolar medium. In them, a nanopool of water or polar solvent is surrounded by the hydrophilic moiety of the surfactant molecules, oriented toward the inner polar solvent whereas the hydrocarbon chains extended towards the bulk non - polar medium [3-4].

Experiments proved that the ternary system of reverse micelles is described as water/oil/surfactant which describes the shape, size, aqueous core structure, solvent effects and microviscosity. The structure and dynamic behavior of water entrapped inside the reverse micelles, distinct significantly from the bulk phase [5]. Particularly, the dynamics of water molecules close to the interface region (hydrophobic) is vital in understanding the convoluted or knotty dynamics in biological environments such as proteins, cell membranes or mitochondria [6]. Various surfactants such as anionic, cationic and zwitter ionic have been adopted to compose RMs. In this regard, the most employed surfactant for formulating anionic RMs is AOT (sodium 1,4 bis 2-ethylhexysulfosuccinate), with a double chain (2–ethylhexyl) hydrophobic tail groups

and a hydrophilic (sulfonate) head group forms stable spherical RMS. The hydrodynamic radius, Rh of AOT RMs is proportional to the molar ratio as [7],

$$Rh = 0.175w + 1.5nm$$

According to reverse micelle swelling law [8], the size of reverse micelles linearly increases with the nonpolar solvent to surfactant ratio W_0 = [polar solvent]/[surfactant]. The water content's size (W_0) in RMs, could influence the size of RMs. For AOT RMs, the W_0 value can be increased upto 40 or more. The size and nature of confined polar solvent (water, for example) of RMs is systematically controlled by varying W_0, virtually all water molecules interact, with the hydrophobic part (head groups) of the surfactant, while free bulk like water emerge as dominant, as W_0 increases [9]. With the aid of molecular probes, it is effective to characterize the RMs and also to examine the water bound therein. In the ternary system (water /oil/surfactant), the probe's locality are constantly discussed, due to solute partition and its reactivity with RMs [10].

The spectroscopic characterization is crucial in finding out probe's locality in RMs. Novaira etal. [11] determined the location of PRODAN (6-Propionyl -2(N,N dimethyl)aminonaphthalene in the AOT RMs using fluorescene and specified the location of PRODAN based on the emission measurements from its intermolecular charge transfer states and their excitations. The photophysical properties of fluorescent dyes in reverse micelles is of great importance, where the fluorescence lifetimes of dyes periodically increases, with respect to the decreased quantum yields within the core of RMs. In RMs, the emission of dyes strongly depends on the locality of fluorophores in heterogeneous reverse micelle system, wherein the dyes with the excited state proton or charge transfer dynamics, strongly depends on the size of the reverse micelles [12].

In these days, researchers are seriously investigating novel methods to trap and remove environmentally harmful dyes from industrial effluents in a cost effective manner [13]. The hydrophobic dyes are trapped by the minute addition of surfactant, which induce the rate of dye adsorption. The changes in spectral features of charged dye-surfactant systems having peculiarity in the dye-surfactant complexes formation, pairs of ions, salts, induced self aggregation of dye, etc. with solubilized monomers of dyes were effectively observed using spectrophotometry, fluorometry, voltammetry, potentiometry and conductometry [14-16]. Surfactant dye interactions are determined by the influence of charge, allyl chain length of surfactants and the substituents location on the aromatic ring of the dye molecule. Based on this strategy, very few have been published so far and accordingly; the interaction of alizarin red dye with surfactants.

Alizarin red, (sodium salt of, 1,2-dihydroxy -9, 10-anthraquinone 3-sulphonic acid) known to be a better candidate for photodynamical therapy, antitumour drug, photosensitizer and also in surfactant-dye interaction, due to its ultrafast excited state intramolecular proton transfer (ESPIT). Herein, we report the three dimensional fluorescence spectral investigations on the interaction of dye-surfactant. AOT, which possess electrostatic and hydrogen bond interactions in head groups [17] and alizarin red has excited state intramolecular proton transfer (ESIPT) makes it more interesting to investigate.

The fundamental aim in this present article is to reveal the photophysical properties of alizarin red such an environment having unique photphysical properties regarding polarity, binding site, binding constant, binding yield etc. Besides this, we have tried to explore the fate of the excited state intramolecular proton transfer (ESIPT) process inside reverse micelles. Finally, we have shown that a more rigid and confined environment inside the reverse micelle is a better model to control the ESIPT process of alizarin red.

Experimental Section

Annals of R.S.C.B., ISSN:1583-6258, Vol. 26, Issue 1, 2022, Pages. 1077- 1092
Received 08 November 2021; Accepted 15 December 2021.

Materials and methods

Sodium salt of 1,2-dihydroxy -9, 10-anthraquinone 3-sulphonic acid (alizarin red dye) and Bis(2-ethylhexyl)sulfosuccinate sodium salt (Aerosol OT, AOT) were purchased from Sigma-Aldrich (Milwaukee, WI, USA) and their molecular structures are given in chart (1) and used without further purification. All other reagents were of HPLC grade and the deionized water used in this work was purified by Milli-Q system. The water/AOT/isooctane reverse micelles were prepared by mixing alizarin red dye solution in water with AOT in isooctane and water is added depending upon the desired molar ratio, W_0 = [water]/[AOT]. Microemulsions of stock solution ($1.5x10^{-4}$ mol dm^{-3}) of dye were prepared by dissolving appropriate amounts in triple distilled water. Other working solutions of surfactant such as AOT stock ($2.4x10^{-3}$ mol dm^{-3}) solution was prepared by dissolving weighted amounts of substance in suitable solvent isooctane.

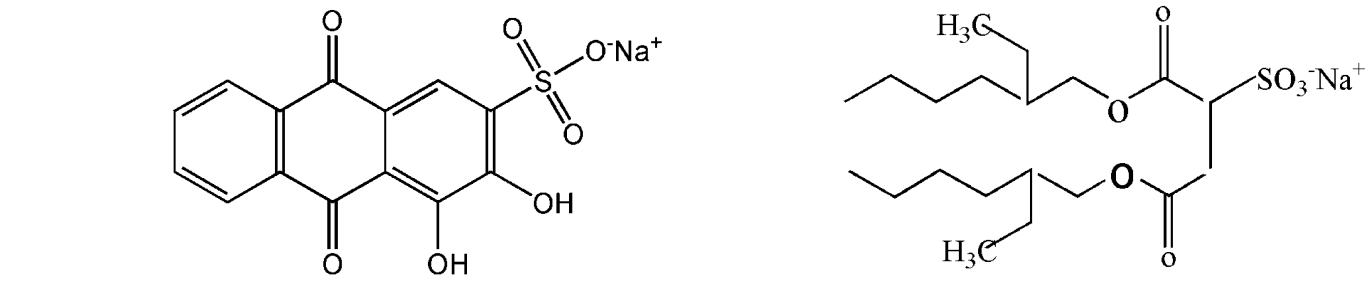

(a) **(b)**

Chart 1. Molecular structure of (a) Alizarin Red dye and (b) Aerosol OT.

UV- Vis absorbance measurement was recorded on a PerkinElmer Lambda 25 UV/VIS spectrophotometer in which matched pair of quartz cells with 1 cm optical length at room temperature in the range of 300-500 nm in the presence and absence of alizarin red dye in the molar ratio concentrations of W_0 = 2, 4, 8, 10, 15, 20, 30, 40, 60.

The fluorescence emission measurements were carried out with FP-8500 JASCO Spectrofluorometer equipped with a xenon lamp and 1 cm path length quartz cuvette. The excitation and emission bandwidths were set at 5 nm and scan rate were kept constant throughout all the measurements. The fluorescence spectra were recorded in the wavelength range of 450-800 nm. 3D fluorescence measurements were analyzed under the fastest scan speed of 60,000 nm m^{-1}.

Results and Discussion

The photophysical properties of the dye in aqueous and non-aqueous solvents are studied. AOT surfactant molecules are dispersed in isooctane, it forms a reverse micelle. When a drop of water is added, wet reverse micelles are formed and the nano waterpool which comprised the inner core of the reverse micelle is characterized by the W_0 values. Since there is a drastic change in the physical properties of the bulk water and the water pool, a probe molecule (say, dye molecule) is used to examine the microenvironment changes as a result of the probe-surfactant interaction. The above mentioned analysis is investigated with the aid of fluorescence spectral technique.

Annals of R.S.C.B., ISSN:1583-6258, Vol. 26, Issue 1, 2022, Pages. 1077- 1092
Received 08 November 2021; Accepted 15 December 2021.

Absorption Spectral Features

UV- Vis and fluorescence spectroscopy could be used to explore the changes in the microenvironment like micelles, reverse micelles, lamellar, biomolecules, biomembranes etc. and to elucidate the interactions of small molecules and provides wealthy information about conformation changes [22,23]. The absorption measurements were recorded for the dye-surfactant solution, with size variation of W_0 = 2, 4, 8, 10, 15, 20, 30, 40, 60. Fig. 1 shows the absorption spectra of alizarin red in water/AOT/isooctane reverse micelles. The absorption spectra in bulk isooctane and in presence of AOT, where the spectra of 1,2-dihydroxy anthraquinone (alizarin), and sodium salt of 1,2-dihydroxy-9,10-anthraquinone-3-sulphonic acid (alizarin red), derivatives of anthraquinone, were clearly distinct due to the presence of sulfonate group, which give soluble aspect to alizarin red. The absorption spectra of neutral alizarin appeared at 250 nm and 430 nm representing the $S_0 \rightarrow S_2$ and $S_0 \rightarrow S_1$ transitions, respectively. With the presence of water loving (sulfonate) group, results from the lowest electronically excited state of unsubstituted anthraquinone lies in the UV- region, due to $n \rightarrow \pi^*$ transitions of *p*–benzoquinone group (diketo form) condensed between two groups. When $n \rightarrow \pi^*$ transitions takes place, the absorption spectral bands were red shifted and these absorption bands of alizarin red occurred at 333 nm and 517 nm. The present probe molecule has two -OH groups as substituents, which enables the electron donating character. The peak appeared at 260nm corresponds to the $n \rightarrow \pi^*$ transition and the peak at 517nm is $\pi \rightarrow \pi^*$ assigned to the intramolecular charge transfer band from the substituent to the aromatic π system.The absorption spectra of alizarin red in AOT reverse micelles is entirely different from that of alizarin red recorded in water. Whereas, the alizarin red is partially soluble in isooctane, the spectral bands appeared at 410 nm, which was nearly similar to spectral bands of water/AOT/isooctane of alizarin red at 436 nm. Since alizarin red is studied, privileged to exist inside the reverse micelles in ternary system. The ternary absorption bands of alizarin red were red shifted at 436 nm showed decrease in intensity in the relatively large (W_0 = 2 – 60) reverse micelles. This may be due to the dye alizarin red exists mainly inside the reverse micelles and the ratios of small reverse micelles than the larger ones. The size of AOT reverse micelles with methanol was estimated as 3- 3.5 nm in diameter (W=1-2) from the DLS measurements [30]. In this regard, the small reverse micelles (polar core) would be more similar or slightly larger than $\sim 1\, nm$ (approximate size) of alizarin red molecule, along with the consideration of tail length (1 nm) of AOT molecules**.** Therefore, it enhances the properties regarding the estimation of alizarin red in small water pool reverse micelles may not fully encapsulated with hydrophilic part of AOT (head groups) due to strong electrostatic interaction. The absorption band occurred at 405 nm represents the ternary system [water/AOT/isooctane], which are distinct from the absorption spectra obtained for reverse micellar solution. In this way, in reverse micelles, the alizarin red at 405 nm (W_0=0) is shifted towards the red end side with increasing W_0 values. It is therefore estimated that the mobility of alizarin red from the bulk isooctane phase to a more polar (hydrophilic) environment, although alizarin red is barely soluble in isooctane, the solubility of molecular probe is considerably increased in the presence of AOT reverse micelles.

Annals of R.S.C.B., ISSN:1583-6258, Vol. 26, Issue 1, 2022, Pages. 1077- 1092
Received 08 November 2021; Accepted 15 December 2021.

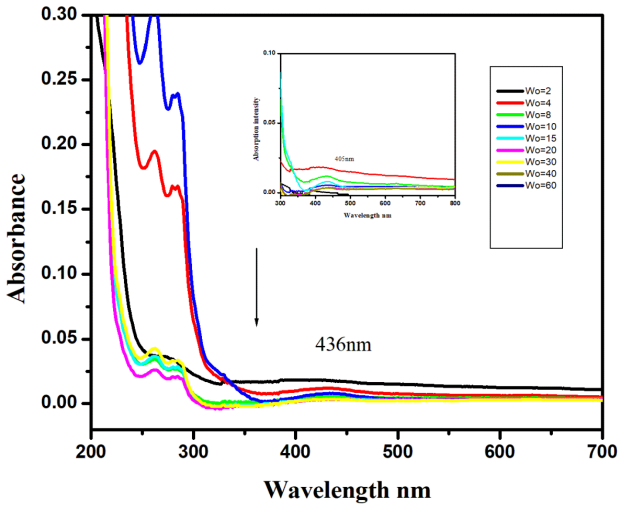

Figure 1. Absorption spectra of Alizarin red at different W_0 values (2-60).

Emission Spectra

The fluorescence spectra of alizarin red in AOT reverse micelles on excitation at 425 nm are shown in Fig.2. The shoulder band shown at 560 nm is the $^{\nu}_{CH}$ Stokes Raman band of isooctane solvent, which is in separable from the broad emission bands [31]. The emission spectrum of alizarin are clearly distinct from the emission of alizarin red as given in Fig. 2 whereas, the emission bands of ternary system [water/AOT/isooctane] were is similar to the emission spectra of alizarin red in water. The emission spectrum of alizarin red in isooctane is also studied and the peaks appeared at 555, 595 and 650nm. The ternary system exhibits two emissive bands at 595 nm and 650 nm due to excited state intramolecular proton transfer (ESIPT). Furthermore, when the size of AOT reverse micelles increase, the emission intensities of alizarin red decreases. It is understood that the nonradiative rate constants of the chromophores of the vibrational relaxation in the excited state are strongly related to the solvent dynamics [13]. When the micelle size increases, results in increasing solvent-solute interactions, which further results in the decrease of chromophores quantum yield [32].

The emission spectrum of alizarin red in large water pool (W_0 = 60) AOT reverse micelles showed a maximum peak at 494 nm with a long tail extended upto700 nm. The emission spectrum for water pool size (W_0 = 60) was slightly different from the emission spectra obtained for alizarin red (water) with the significant spectral contribution of alizarin red spectrum (isooctane). However the existence of alizarin red in distinct water nanopool AOT reverse micelles was confirmed in both absorption and emission measurements. When ternary system interacts, these emission bands exhibit a slight red shift at 500 nm. Furthermore, the increase in the nanopool size of the reverse micelles results in the enhancement of emission intensity. The emission spectrum occurred at 595 nm gradually diminishes due to the decreasing concentration of alizarin red in isooctane with increasing size of nano waterpools (W_0**)** [33]. The peculiar emission spectrum obtained (inset Fig. 2) clearly depicts the appearance of the 653 nm emission band in the reverse micelles, due to the molecular probe mobility during solute-solvent interactions. In this regard, the difference in the emission spectra of alizarin red in the ternary system [water/AOT/isooctane] compared to the alizarin red in isooctane (bulk phase) may also be attributed due to the confined reverse micellar environment evident from thechange in the emission profile of alizarin red. Furthermore, the additional excited state processes such as inter

Annals of R.S.C.B., ISSN:1583-6258, Vol. 26, Issue 1, 2022, Pages. 1077- 1092
Received 08 November 2021; Accepted 15 December 2021.

system crossing (ISC) to the triplet state may occur in reverse micelles, which have the ability to enhance the lifetime of alizarin red effectively. On increasing W_0 values, the fluorescence intensity increased with a considerable bathochromic shift (30nm) as highlighted in the inset Fig. 2, due to the formation of Alizarin red –AOT complex association with the polar region of the reverse micelles.

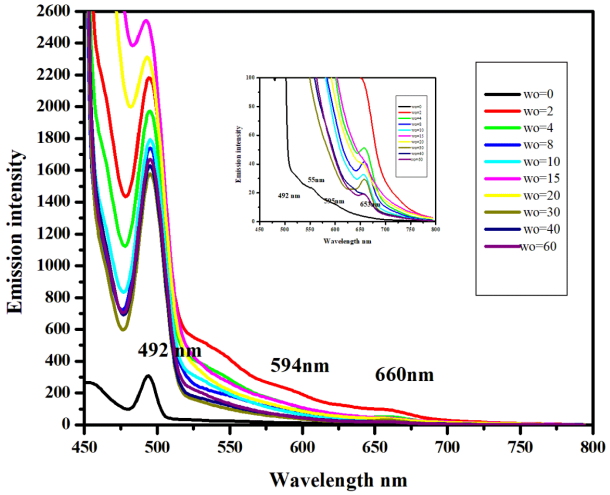

Figure 2. Emission spectra of Alizarin red with various W_0 values (0-60).

Determination of Excited state pKa

At different pH, the emission intensity values are measured and plotted against the pH of the solutions (Figure 3). The resulting data were fit into the sigmoidal curve, the inflection point were calculated. The titration curve shows the excited state pKa value be equal to 6 which presumably corresponds to the protonation of the carbonyl group (C=O) in Alizarin red dye [34,35].

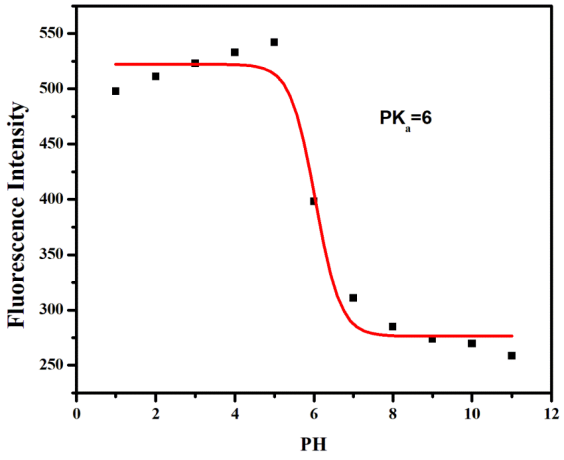

Figure 3. . Plot of pH against fluorescence intensity of Alizarin red dye.

Evaluation of Binding parameters

Annals of R.S.C.B., ISSN:1583-6258, Vol. 26, Issue 1, 2022, Pages. 1077- 1092
Received 08 November 2021; Accepted 15 December 2021.

When small molecules bind independently to a set of equivalent sites on the macromolecules, the interaction can be analysed using Benesi-Hildebrand equation. The modified Benesi -Hildebrand equation [36, 37] gives an idea about the binding between dye – surfactant interactions. Hence, the titration data is exploited to determine the binding pattern of dye –surfactant systems using the following equation.

$$\frac{1}{\Delta F} = \frac{1}{\Delta F_{max}} + \frac{1}{K\Delta F_{max}} \frac{1}{[Surfactant]^n}$$

where $\Delta F=F_x-F_0$ and $\Delta F_{max}=F_\infty-F_0$, F_0, F_x, and F_∞ are fluorescence intensities of dye in absence of AOT , at intermediate AOT concentration and final AOT concentration. K and n denotes the binding constant and stochiometric coefficient.

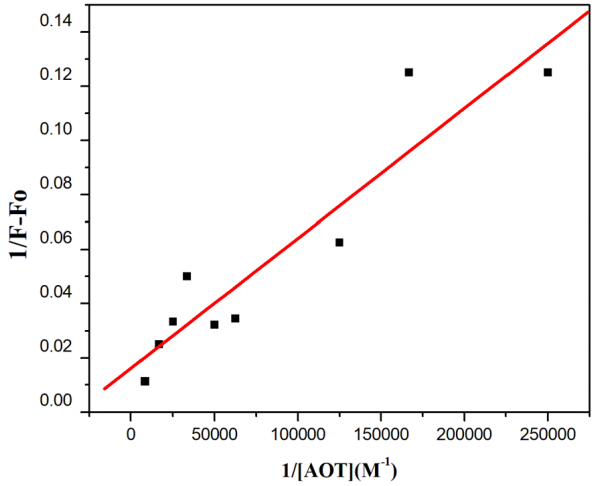

Figure 4. Double reciprocal plot for the interaction of Alizarin red with AOT reverse micelles.

.

Plot of 1/ΔF Vs 1/[AOT] gives a straight line, and the binding constant is $3.395x10^4M^{-1}$. Modified Stern Volmer
equation was used for calculating the number of binding sites at dye molecule and binding constant of dye-surfactant system as shown below [38, 39].

$$\log \frac{F - F0}{F} = logK' + \beta \log [AOT]$$

where F_0 and F denote the fluorescence intensities in the absence and presence of surfactant, K' is the binding constant and β is the binding affinity, i.e., the number of surfactant molecules interacting per site. Plot of log $(F-F_0)/F$ vs log [AOT] gives a straight line and the number of binding sites β is approximately 1(0.9358).

Annals of R.S.C.B., ISSN:1583-6258, Vol. 26, Issue 1, 2022, Pages. 1077- 1092
Received 08 November 2021; Accepted 15 December 2021.

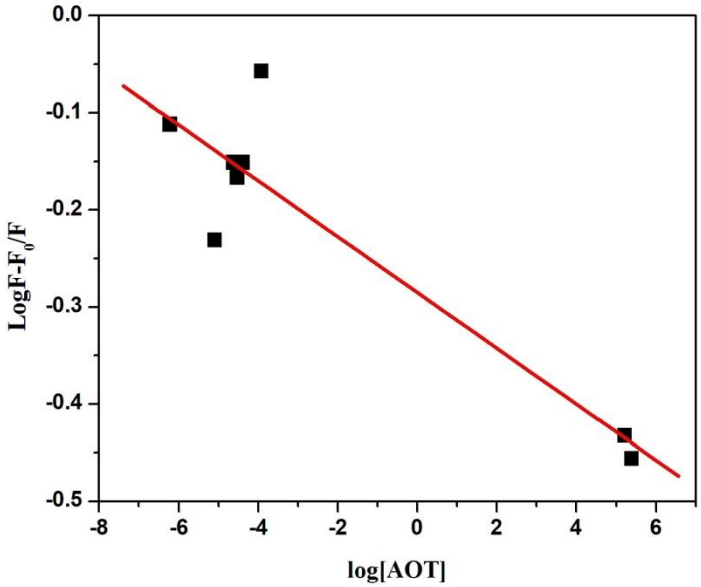

Figure 5. Modified Stern Volmer plot for interaction of Alizarin red with AOT reverse micelles.

Determination of Partition Co-efficient

The partition co-efficient can be determined from the change in the fluorescence intensity of the probe with the surfactant concentration measured at a particular wavelength. If the analytical probe molecule is kept constant and the absorbance of the sample at the working excitation wavelength is low [40, 41]the following equation can be deduced,

$$I = I_0 (\varphi_f + \varphi_b K_p [AOT])/ (1+ K_p[AOT])$$

where I_0 is the intensity of incident light, I is the fluorescence intensity measured at the surfactant concentration considered, φ_f and φ_b are the fluorescent quantum yields of alizarin red in organic solvent and bound to the reverse micelle interface, respectively. The plot for the determination of partition constant is shown in Figure 6 and the value of partition constant (K_p) was found to be $6.5x10^4$.

Annals of R.S.C.B., ISSN:1583-6258, Vol. 26, Issue 1, 2022, Pages. 1077- 1092
Received 08 November 2021; Accepted 15 December 2021.

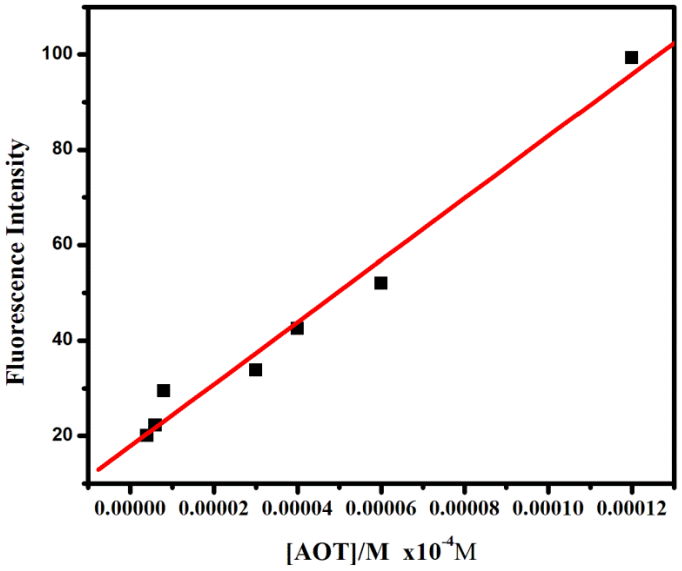

Figure 6. Plot of fluorescence intensity versus [AOT] reverse micelles.

3D Fluorescence Spectroscopy

Conformational changes of microenvironment, reverse micelles are studied by a new proposed analytical technique, 3D fluorescence spectroscopy [42]. The three dimensional axes (excitation wavelength, emission wavelength and fluorescence intensity) paved the way to investigate the characteristic conformational changes of surfactants within the microenvironment in a more scientific and conclusive way [43]. The contour map set forth a bird's eye view of fluorescence spectra, which impart a lot of important informations [44]. Three characteristics excitation/emission peaks for Alizarin red are identified on the 3D fluorescence spectrum (Fig.7) with centers located at, $\lambda_{ex}/\lambda_{em}$ = 460/555 nm, $\lambda_{ex}/\lambda_{em}$ = 460/594 nm and $\lambda_{ex}/\lambda_{em}$ = 460/650nm. Peak 1($\lambda_{ex}/\lambda_{em}$ = 420/555 nm) corresponds to n→π* character of unsubstituted anthraquinone. As referred to peak 2 and peak 3, revealed the spectral characteristic of Alizarin red in normal form and phototautomer form, when it is excited at 420 nm.

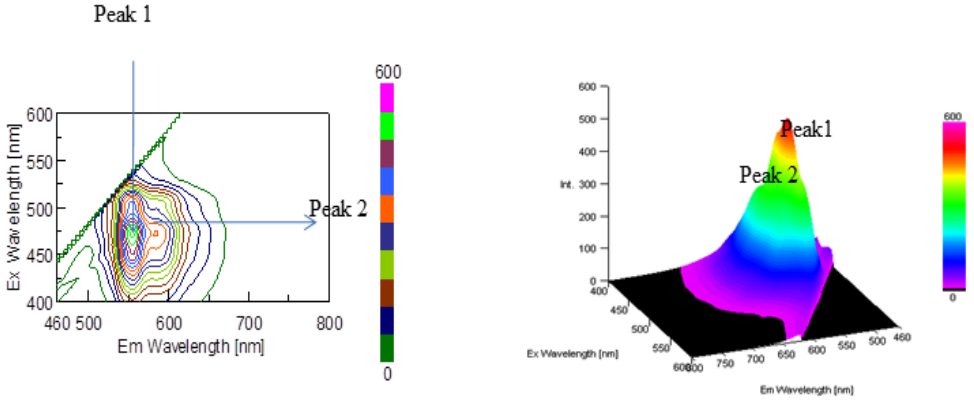

Annals of R.S.C.B., ISSN:1583-6258, Vol. 26, Issue 1, 2022, Pages. 1077- 1092
Received 08 November 2021; Accepted 15 December 2021.

Figure 7. Contour and 3D fluorescence spectra of Alizarin red in isoctane(W_0 = 0)

Interaction of Alizarin red in Reverse micelles

Figure (7-13) represents the contour and three dimensional spectra of Alizarin red in different W_0 values (W_0 = 2-60). Three characteristic excitation/emission peaks for Alizarin red in W_0 = 2 were identified on the 3D spectrum (Fig.8), with the centres located at peak 1 $\lambda_{ex}/\lambda_{em}$ = 560/595nm, and peak 2 $\lambda_{ex}/\lambda_{em}$ = 560/660nm and the intensity of peak 1 is much stronger than peak 2. The high energy emission (absorption) at 260nm is due to n→π* transitions of the unsubstituted anthraquinone and the low energy emission (absorption) at 436nm is due to π→π* transitions assigned to the intramolecular charge transfer from the substituent to the aromatic π system. Peak A is the Rayleigh scattering peak 545/545→600/600 nm (λ_{ex} = λ_{em}). It can be seen that the fluorescence intensity of peak A (scattering peak) increased with increase the size of the water pool (W_0 = 0-60), the possible explanation may be that a Alizarin red-AOT complex came into being after the addition of AOT with the increase in the diameter of water pool, which in turn resulted in the enhancement of the scattering effect in fig.10 [45]. The fluorescence intensity of the peak 1 and 2 decreased markedly due to the quenching of Alizarin red in AOT, W_0 values (2-60), which further demonstrated the fluorescence quenching in the binding process and the maximum emission wavelength of the peak 2 in (fig .13) have obvious red shift (650nm→670nm) followed by increasing W_0 values as a result of formation of Alizarin red – AOT complex association with the polar region of the reverse micelles. This detection could be spelt out in light of certain models of the waterpool microenvironment. When the water pool grows up, all the Alizarin red molecules may be completely localized in the inner core region of the AOT reverse micelles as evident from the red shift [46]. The entire above phenomenon and the analysis of fluorescence characteristics of the peaks revealed that the binding of Alizarin red with reverse micelles (AOT) induced some micro environmental changes in reverse micelles.

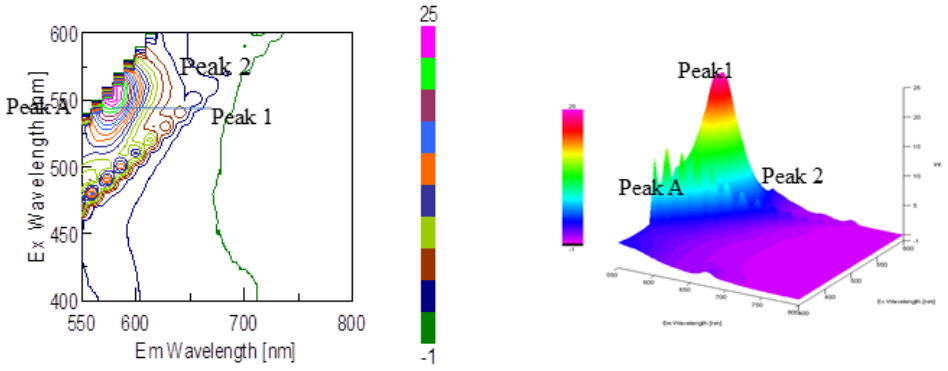

Figure 8. Contour map and 3D fluorescence spectra of Alizarin red in AOT(W_0 = 2).

Annals of R.S.C.B., ISSN:1583-6258, Vol. 26, Issue 1, 2022, Pages. 1077- 1092
Received 08 November 2021; Accepted 15 December 2021.

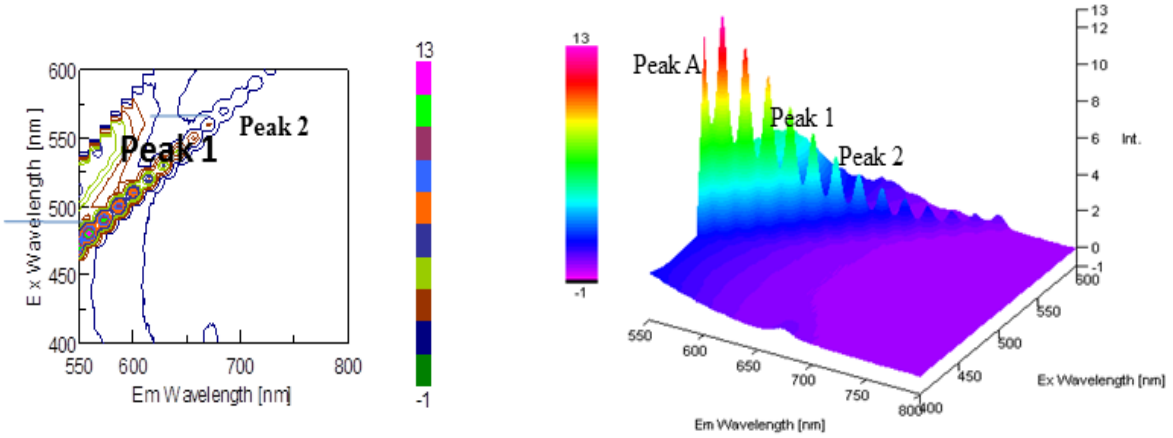

Figure 9. Contour map and 3D fluorescence spectra of Alizarin red in AOT (W_0 = 4).

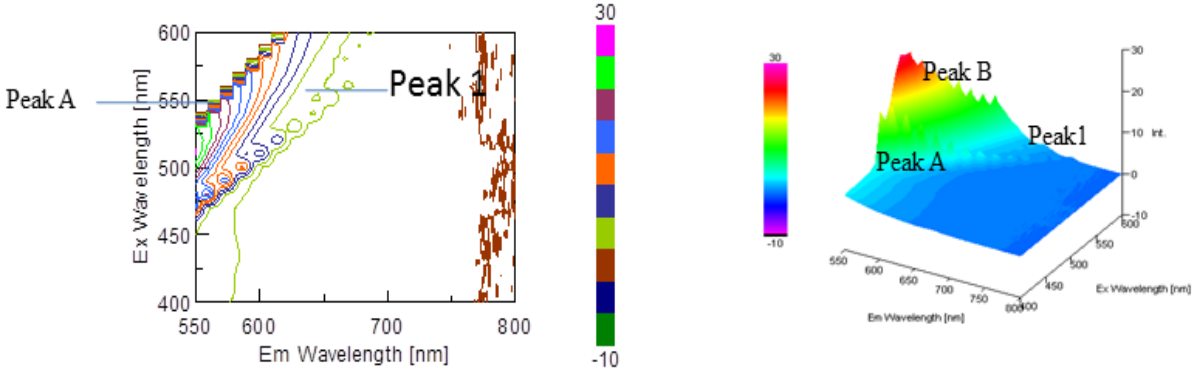

Figure 10. Contour map and 3D fluorescence spectra of Alizarin red in AOT (W_0 = 8).

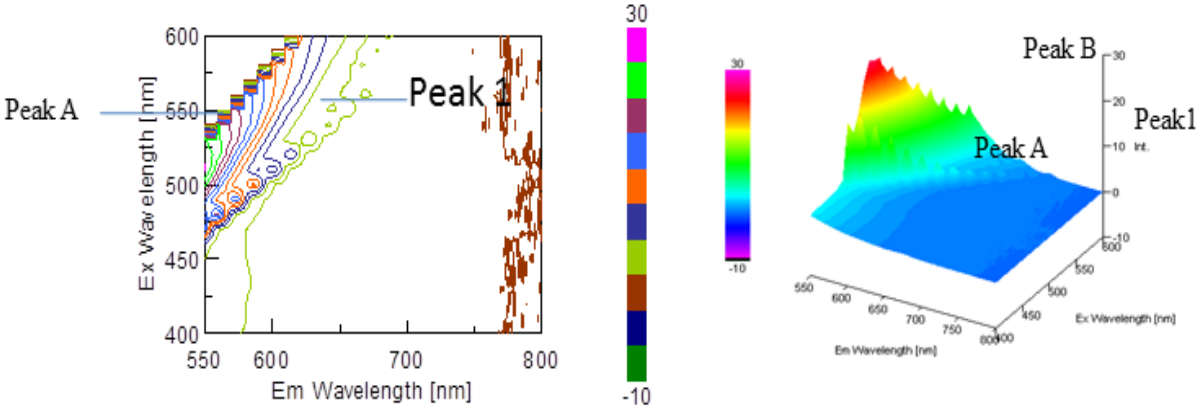

Figure 11. Contour map and 3D fluorescence spectra of Alizarin red in AOT (W_0 = 15).

Annals of R.S.C.B., ISSN:1583-6258, Vol. 26, Issue 1, 2022, Pages. 1077- 1092
Received 08 November 2021; Accepted 15 December 2021.

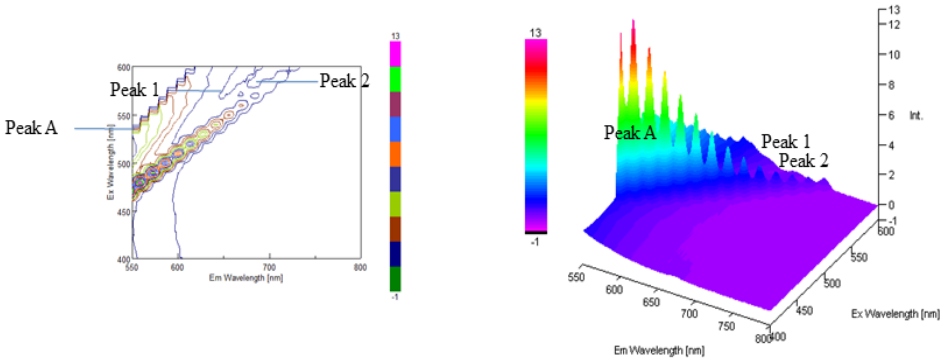

Figure 12. Contour map and 3D fluorescence spectra of Alizarin red in AOT (W_0 = 40).

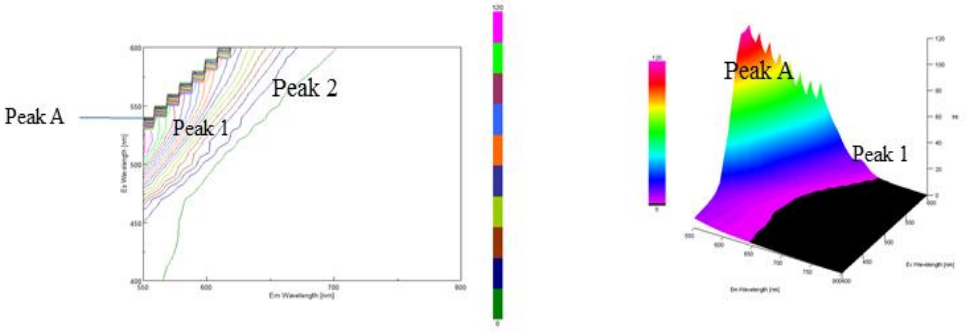

Figure 13. Contour map and 3D fluorescence spectra of Alizarin red in AOT (W_0 = 60).

Conclusion

In conclusion, the results reported here highlighted the detailed information about the photophysical properties of the spectroscopic probe Alizarin Red, a molecule showing the ESIPT process in aqueous and non aqueous AOT reverse micelles. The remarkable enhancement in fluorescence intensity with a distinct red shift along with 3D fluorescence spectrum dictate the formation of Alizarin red dye-AOT complex association with the polar region of the reverse micelles. In accordance with emission intensity changes, the value of binding constant is $3.395 \times 10^4 M^{-1}$ and the binding site is ~ equal to 1 (0.9358). The quantum yield is found to be 0.074 and the partition constant is calculated to be 6.5×10^4. From the experiments, it is possible to control the emission properties of Alizarin red by tuning the W_0 values. Moreover these reverse micelle systems can be a good models to study the processes that occur within the biological macromolecules embedded in biological membranes.

References

[1] Fendler, J. H. (1980). Microemulsions, micelles, and vesicles as media for membrane mimetic photochemistry. *The Journal of Physical Chemistry*, *84*(12), 1485-1491.

[2] Riter, R. E., Undiks, E. P., & Levinger, N. E. (1998). Impact of counterion on water motion in aerosol OT reverse micelles. *Journal of the American Chemical Society*, *120*(24), 6062-6067.

[3] Deàk, J. C., Pang, Y., Sechler, T. D., Wang, Z., & Dlott, D. D. (2004). Vibrational energy transfer across a reverse micelle surfactant layer. *Science*, *306*(5695), 473-476.
[4] Lawler, C., & Fayer, M. D. (2015). Proton transfer in ionic and neutral reverse micelles. *The Journal of Physical Chemistry B*, *119*(19), 6024-6034.
[5] Levinger, N. E. (2000). Ultrafast dynamics in reverse micelles, microemulsions, and vesicles. *Current opinion in colloid & interface science*, *5*(1-2), 118-124.
[6] Nandi, N., Bhattacharyya, K., & Bagchi, B. (2000). Dielectric relaxation and solvation dynamics of water in complex chemical and biological systems. *Chemical Reviews*, *100*(6), 2013-2046.
[7] Fuglestad, B., Gupta, K., Wand, A. J., & Sharp, K. A. (2019). Water loading driven size, shape, and composition of cetyltrimethylammonium/hexanol/pentane reverse micelles. *Journal of colloid and interface science*, *540*, 207-217.
[8] Dib, N., Falcone, R. D., Acuña, A., & García-Río, L. (2019). Characterization of Reverse Micelles Formulated with the Ionic-Liquid-like Surfactant Bmim-AOT and Comparison with the Traditional Na-AOT: Dynamic Light Scattering, 1H NMR Spectroscopy, and Hydrolysis Reaction of Carbonate as a Probe. *Langmuir*, *35*(39), 12744-12753.
[9] Lee, G., Jang, T., Lee, S., Oh, H., Lee, H., & Pang, Y. (2020). Excited-state dynamics of 4-dimethylamino-4′-nitrobiphenyl confined in AOT reverse micelles. *Journal of Molecular Liquids*, *305*, 112873.
[10] Małycha, K., Pocheć, M., & Orzechowski, K. (2019). Non-linear dielectric effect in reverse micelles system. *Journal of Molecular Liquids*, *291*, 111344.
[11] Sakai, H., Harada, M., & Okada, T. (2020). Reverse micelle chromatography for evaluation of partition of organic solutes to micellar pseudophases. *Journal of Colloid and Interface Science*, *577*, 191-198.
[12] Sun, X., & Bandara, N. (2019). Applications of reverse micelles technique in food science: A comprehensive review. *Trends in Food Science & Technology*, *91*, 106-115.
[13] Jang, T., Lee, G., Lee, S., Lee, J., & Pang, Y. (2019). Photophysical properties of 1, 2-dihydroxyanthraquinone in AOT reverse micelles. *Journal of Molecular Liquids*, *279*, 503-509.
[14] Ridley, R. E., Alvarado, E., Mrse, A. A., Vasquez, V. R., & Graeve, O. A. (2020). Phase Stability and Miscibility in Ethanol/AOT/n-Heptane Systems: Evidence of Multilayered Cylindrical and Spherical Microemulsion Morphologies. *Langmuir*, *36*(38), 11274-11283.
[15] Lépori, C. M., Correa, N. M., Silber, J. J., Falcone, R. D., López-López, M., & Moyá, M. L. (2020). Influence of the AOT Counterion Chemical Structure on the Generation of Organized Systems. *Langmuir*, *36*(36), 10785-10793.
[16] Sun, X., & Bandara, N. (2019). Applications of reverse micelles technique in food science: A comprehensive review. *Trends in Food Science & Technology*, *91*, 106-115.
[17] Crans, D. C., Rithner, C. D., Baruah, B., Gourley, B. L., & Levinger, N. E. (2006). Molecular probe location in reverse micelles determined by NMR dipolar interactions. *Journal of the American Chemical Society*, *128*(13), 4437-4445.
[18] Novaira, M., Moyano, F., Biasutti, M. A., Silber, J. J., & Correa, N. M. (2008). An example of how to use AOT reverse micelle interfaces to control a photoinduced intramolecular charge-transfer process. *Langmuir*, *24*(9), 4637-4646.
[19] K. Salem, M. Issa, E. Nahhal, S.F. Salama, Chem.Phy.Letters., 730, 445-450 (2019).
[20] Sasirekha, V., Umadevi, M., & Ramakrishnan, V. (2008). Solvatochromic study of 1, 2-dihydroxyanthraquinone in neat and binary solvent mixtures. *Spectrochimica Acta Part A: Molecular and Biomolecular Spectroscopy*, *69*(1), 148-155.

[21] Sarkar, M., & Poddar, S. (1999). Spectral studies of methyl violet in aqueous solutions of different surfactants in supermicellar concentration region. *Spectrochimica Acta Part A: Molecular and Biomolecular Spectroscopy*, *55*(9), 1737-1742.

[22] Wang, Q., Huang, C. R., Jiang, M., Zhu, Y. Y., Wang, J., Chen, J., & Shi, J. H. (2016). Binding interaction of atorvastatin with bovine serum albumin: Spectroscopic methods and molecular docking. *Spectrochimica Acta Part A: Molecular and Biomolecular Spectroscopy*, *156*, 155-163.

[23] Wang, J., Ma, L., Zhang, Y., & Jiang, T. (2017). Investigation of the interaction of deltamethrin (DM) with human serum albumin by multi-spectroscopic method. *Journal of Molecular Structure*, *1129*, 160-168.

[24] Pandit, P., & Basu, S. (2004). Removal of ionic dyes from water by solvent extraction using reverse micelles. *Environmental science & technology*, *38*(8), 2435-2442.

[25] Khan, M. N., & Sarwar, A. (2006). Study of dye–surfactant interaction: aggregation and dissolution of yellowish in N-dodecyl pyridinum chloride. *Fluid Phase Equilibria*, *239*(2), 166-171.

[26] Sanan, R., Kang, T. S., & Mahajan, R. K. (2014). Complexation, dimerisation and solubilisation of methylene blue in the presence of biamphiphilic ionic liquids: a detailed spectroscopic and electrochemical study. *Physical Chemistry Chemical Physics*, *16*(12), 5667-5677.

[27] Kurniasih, I. N., Liang, H., Mohr, P. C., Khot, G., Rabe, J. P., & Mohr, A. (2015). Nile red dye in aqueous surfactant and micellar solution. *Langmuir*, *31*(9), 2639-2648.

[28] Simončič, B., & Kert, M. (2006). Thermodynamics of anionic dye–cationic surfactant interactions in cationic–nonionic surfactant mixtures in comparison with binary systems. *Dyes and pigments*, *71*(1), 43-53.

[29] Asadzadeh Shahir, A., Javadian, S., Razavizadeh, B. B. M., & Gharibi, H. (2011). Comprehensive study of tartrazine/cationic surfactant interaction. *The Journal of Physical Chemistry B*, *115*(49), 14435-14444.

[30] Riter, R. E., Kimmel, J. R., Undiks, E. P., & Levinger, N. E. (1997). Novel reverse micelles partitioning nonaqueous polar solvents in a hydrocarbon continuous phase. *The Journal of Physical Chemistry B*, *101*(41), 8292-8297.

[31] Lee, S., Lee, J., & Pang, Y. (2015). Excited state intramolecular proton transfer of 1, 2-dihydroxyanthraquinone by femtosecond transient absorption spectroscopy. *Current Applied Physics*, *15*(11), 1492-1499.

[32] Maity, B., Chatterjee, A., & Seth, D. (2014). The photophysics of 7-(diethylamino) coumarin-3-carboxylic acid N-succinimidyl ester in reverse micelle: excitation wavelength dependent dynamics. *RSC Advances*, *4*(7), 3461-3471.

[33] Banerjee, C., Ghatak, C., Mandal, S., Ghosh, S., Kuchlyan, J., & Sarkar, N. (2013). Curcumin in reverse micelle: An example to control excited-state intramolecular proton transfer (esipt) in confined media. *The Journal of Physical Chemistry B*, *117*(23), 6906-6916.

[34] Miyata, S., Hoshino, M., Isozaki, T., Yamada, T., Sugimura, H., Xu, Y. Z., & Suzuki, T. (2018). Acid Dissociation Equilibrium and Singlet Molecular Oxygen Quantum Yield of Acetylated 6, 8-Dithioguanosine in Aqueous Buffer Solution. *The Journal of Physical Chemistry B*, *122*(11), 2912-2921.

[35] Ioele, M., Bazzanini, R., Chatgilialoglu, C., & Mulazzani, Q. G. (2000). Chemical radiation studies of 8-bromoguanosine in aqueous solutions. *Journal of the American Chemical Society*, *122*(9), 1900-1907.

[36] Benesi, H. A., & Hildebrand, J. H. J. (1949). A spectrophotometric investigation of the interaction of iodine with aromatic hydrocarbons. *Journal of the American Chemical Society*, *71*(8), 2703-2707.

[37] Sanan, R., Kang, T. S., & Mahajan, R. K. (2014). Complexation, dimerisation and solubilisation of methylene blue in the presence of biamphiphilic ionic liquids: a detailed spectroscopic and electrochemical study. *Physical Chemistry Chemical Physics*, *16*(12), 5667-5677.

[38] Sahoo, D., Bhattacharya, P., & Chakravorti, S. (2010). Quest for mode of binding of 2-(4-(dimethylamino) styryl)-1-methylpyridinium iodide with calf thymus DNA. *The Journal of Physical Chemistry B*, *114*(5), 2044-2050.

[39] Maltas, E. (2014). Binding interactions of niclosamide with serum proteins. *journal of food and drug analysis*, *22*(4), 549-555.

[40] Beare, M. H., Coleman, D. C., Crossley, D. A., Hendrix, P. F., & Odum, E. P. (1995). A hierarchical approach to evaluating the significance of soil biodiversity to biogeochemical cycling. In *The significance and regulation of soil biodiversity* (pp. 5-22). Springer, Dordrecht.

[41] Baritrop, J. A., Coyle, J. D., & Klerer, J. (1979). Principles of Photochemistry. *Journal of The Electrochemical Society*, *126*(12), 492C.

[42] Tan, L., Liu, L., Xie, Q., Zhang, Y., & Yao, S. (2004). Fluorescence quenching of bovine serum albumin in reversed micelles by CdS nanoparticles. *Analytical sciences*, *20*(3), 441-444.

[43] He, L., Wang, X., Liu, B., Wang, J., Sun, Y., Gao, E., & Xu, S. (2011). Study on the interaction between promethazine hydrochloride and bovine serum albumin by fluorescence spectroscopy. *Journal of Luminescence*, *131*(2), 285-290.

[44] Li, D., Zhu, M., Xu, C., & Ji, B. (2011). Characterization of the baicalein–bovine serum albumin complex without or with Cu2+ or Fe3+ by spectroscopic approaches. *European Journal of Medicinal Chemistry*, *46*(2), 588-599.

[45] Li, D., Wang, Y., Chen, J., & Ji, B. (2011). Characterization of the interaction between farrerol and bovine serum albumin by fluorescence and circular dichroism. *Spectrochimica Acta Part A: Molecular and Biomolecular Spectroscopy*, *79*(3), 680-686.

[46] Tan, L., Liu, L., Xie, Q., Zhang, Y., & Yao, S. (2004). Fluorescence quenching of bovine serum albumin in reversed micelles by CdS nanoparticles. *Analytical sciences*, *20*(3), 441-444.